N 73 27410

NASA TECHNICAL MEMORANDUM

NASA TM X-68260

NASA TM X-68260

CASE FILE COPY

CORRELATION OF MAGNETIC PERTURBATION INSPECTION DATA WITH ROLLING-ELEMENT BEARING FATIGUE RESULTS

by R. J. Parker
Lewis Research Center
Cleveland, Ohio

TECHNICAL PAPER proposed for presentation at
Joint Lubrication Conference cosponsored by the
American Society of Lubrication Engineers and the
American Society of Mechanical Engineers
Atlanta, Georgia, October 16-18, 1973

CORRELATION OF MAGNETIC PERTURBATION INSPECTION DATA WITH ROLLING-ELEMENT BEARING FATIGUE RESULTS

by R. J. Parker[1]

NASA, Lewis Research Center, Cleveland, Ohio

E-7549

ABSTRACT

A magnetic perturbation technique was used to nondestructively detect subsurface nonmetallic inclusions in the inner races of 207-size, deep groove ball bearings. The bearings were fatigue tested at 2750 rpm under a radial load of 5860 newtons (1320 lb). The inner races were subsequently sectioned at fatigue spall locations and at magnetic perturbation signal locations. Analyses of the data indicated good correlation between magnetic perturbation signals and inclusion size and location. Exclusion of those bearings that had significant magnetic perturbation signals did not alter the statistical life of the bearings.

INTRODUCTION

Fatigue spalls in rolling-element bearings can be initiated at nonmetallic inclusions in the bearing steels [1 to 5][2]. In the concentrated contact between rolling-elements, inclusions near the rolling surface act as stress concentrations. Fatigue cracks nucleate at these inclusions, and propagate under repeated stresses to form a network of cracks which eventually forms a fatigue spall. Such inclusions are not the sole source of stress concentration which originate rolling-element fatigue cracks.

---

[1]Member ASME.

[2]Numbers in brackets designate references at the end of the paper.

Other stress concentrations include: large or unusual carbide formations; surface flaws such as debris dents, grinding furrows, skids, and corrosion pits; misalinement and edge loading of rollers. However, subsurface inclusions are the dominant stress raisers at which fatigue cracks originate [5].

The location, size and type of nonmetallic inclusion are important in the initiation of fatigue cracks. Generally, only those inclusions at the surface and in the near subsurface zone of high shear stress have been found to initiate fatigue cracks that propagate and develop into fatigue spalls [3]. Although there is some evidence of fatigue crack initiation at very small inclusions, most evidence of fatigue crack initiation is from the larger inclusions [4, 5]. The hard, nonmetallic inclusions, such as oxides, or aluminas, are found to be significant stress raisers whereas the softer sulfide inclusions have generally shown no detrimental effects [5].

Initially, rolling-element bearing steels were produced by basic electric arc melting. Within the last 10 to 15 years, vacuum-melting processes such as carbon vacuum degassing and consumable-electrode vacuum-melting have significantly reduced the nonmetallic inclusion count from that of the earlier materials. Even in exceptionally clean materials, nonmetallic inclusions are present to some degree and, depending on their size and location can be the nucleus of fatigue cracks as a result of the repeated stressing in rolling contact. Accordingly, nondestructive inspections are used in the bearing industry to eliminate those bearing components containing flaws. The most widely used method,

magnetic particle [6, 7], is capable of finding larger flaws and those penetrating the surface, but it is not sensitive enough to find the very small flaws, approximately 0.0025 to 0.0075 centimeters (0.001 to 0.003 in.) in diameter that often cause bearing fatigue failures. Therefore, in applications of rolling-element bearings where very high reliability is required, a nondestructive inspection method that would detect harmful nonmetallic inclusions in critical areas of the bearing components would be a valuable tool. More reliable bearings could be assembled with bearing components that show no significant inclusions in this inspection.

Magnetic perturbation is a nondestructive inspection method that detects the presence, location, and size of nonmetallic inclusions, voids, and local metallurgical inhomogeneities in ferromagnetic materials [8-11]. The capability of this method for detecting the very small, nonmetallic inclusions at the surface and within the first few mils of depth in rolling-element bearing steels has previously been reported [12, 13].

The research reported herein, which is based on the work reported initially in [12 and 14], was undertaken to investigate the correlation between magnetic perturbation results and rolling-element fatigue. The objectives were to (a) inspect inner-races of 207-size, deep-groove ball bearings by magnetic perturbation and document significant inclusions, (b) fatigue test sufficient numbers of these bearings and compare the results with the inspection measurements, and (c) determine the relation between the magnetic perturbation results and the location and size of nonmetallic inclusions as determined by metallurgical sectioning.

APPARATUS AND PROCEDURE

Magnetic Perturbation Method

The fact that voids, inclusions, local metallurgical structure inhomogeneities, and local stresses can influence the configuration of magnetic domains is the basis of the magnetic perturbation method [8-13, 15-24]. The method essentially consists of establishing a magnetic flux in the region of the material being inspected, and then scanning the surface of the material with a sensitive magnetic probe to detect anomalies or perturbations in the magnetic flux. Figure 1 schematically illustrates this concept. The flux lines are relatively uniform and parallel in regions remote from the flaw or inclusion. In the vicinity of the inclusion, the flux lines are distorted or perturbed. This perturbation causes flux lines to emerge and re-enter the material surface. The intensity of the perturbation is influenced by the flaw size and depth beneath the surface, the applied magnetic flux, and the overall magnetic properties of the material being examined.

Bearing Race Inspection

A schematic diagram of the magnetic perturbation method adapted for bearing inner-race inspection is presented in figure 2. The race is magnetized as shown in figure 2(a). Surface and subsurface locally varying magnetic regions produce perturbations in the magnetic flux at the surface of the race as shown in figure 2(b). A probe scans the surface as the race is rotated (fig. 2(c)). Characteristic signals or signatures are produced by defects such as inclusions, pits, dents, or corrosion. The position of defects as small as 0.0025 centimeter (0.001 in.) in diameter can be located.

Magnetic perturbation inspection records were obtained on 100 inner races before endurance testing. On each race a total of ten adjacent inspection tracks approximately 0.064 centimeter (0.025 in.) wide with a slight overlap on adjacent tracks were made. The center of the scan region was coincident with the centerline of the bearing, and inspection tracks were centered at 2.5°, 357.5°, 7.7°, 352.2°, 13.0°, 347.0°, 18.2°, 341.7°, 23.5°, and 336.5°.

After visual analysis of the records, specific regions on a number of specimens were re-inspected, magnetically, and expanded sweep photographs of signatures were obtained. These expanded sweep records permit a more detailed evaluation of the signature source. In addition, photomicrographs of the race surface at approximately ×50 magnification were obtained at the location of the signals on most of these races.

After endurance testing, magnetic perturbation inspections were accomplished in a manner similar to those obtained prior to endurance testing, except when severe spalling of a raceway had occurred. The surfaces were examined at ×50 and ×100 magnification for signs of cracking at signal locations.

Test Bearings

The inner races investigated in this program were taken from 207-size deep-groove ball bearings of ABEC grade 5. The inner races were from one heat of air-melted, vacuum-degassed AISI 52100 steel. Rockwell C hardness of the inner races was 62.0 to 62.5. The balls were AFBMA grade 10, made from another heat of AISI 52100 and hardened to Rockwell C 63.5 to 64.0.

Of the 100 bearing inner races, only 54 could be used for fatigue testing because of the availability of a suitable set of outer races. The 54 assembled bearings included the 20 inner races with the largest and most critically located signals associated with voids and/or inclusions.

Bearing Fatigue Tests

These fifty-four bearings were the identical bearings that were used for the prestessing study reported in [14]. This prestressing study involved the fatigue testing of two groups of 27 bearings per group. One group was subjected to a prestress cycle prior to fatigue testing but after the magnetic perturbation inspection. This cycle consisted of running the bearing at 2750 rpm for 25 hours under a radial load producing a maximum Hertz stress of 3.3×10^9 newtons per meter squared (480 000 psi) at the inner-race-ball contact. The other group of 27 bearings was not subjected to the prestress cycle.

All 54 bearings were fatigue tested in a test rig capable of simultaneously running four bearings at 2750 rpm under a radial load of 5860 newtons (1320 lb), a maximum Hertz stress of 2.4×10^9 newtons per meter squared (350 000 psi) at the inner-race-ball contact, and jet lubricated with a super-refined naphthenic mineral oil. Bearing outer-race temperature was 339 to 344 K (150° to 160° F).

Each bearing was run until fatigue failure or until a preset cutoff time was reached. This cutoff time was 4000 hours (6.6×10^8 cycles) for the baseline bearings and 10 000 hours (16.5×10^8 cycles) for the prestressed bearings. The prestressed bearings had a 10 percent fatigue life at least twice that of the 27 baseline bearings [14].

RESULTS AND DISCUSSION

Magnetic Perturbation Inspection Results

Analysis of the magnetic inspection records disclosed 23 out of the total of 100 inner races with signals associated with voids and/or inclusions. In figure 3 inspection records with typical inclusion signatures indicated by arrows are shown. Figure 3(c) is an exception since the "polarity" is opposite of that for an inclusion, but this signature is presented to illustrate discrimination of the method. It is noted that this signal when examined from left to right first goes upward and then downward, whereas the signal typical of an inclusion or void first goes downward and then upward. Typical expanded sweep records are presented in figure 4. The signature from specimen number 11 is opposite in polarity from an inclusion signal and therefore is not from an inclusion. Table I shows typical data taken from the magnetic perturbation records for several bearing races that were tested.

Fatigue Results

Fatigue life results are shown in the Weibull plots of figure 5 for the two groups of baseline and the prestressed bearings. Of the 27 bearings in each group, 10 in each group showed magnetic perturbation signals which indicate the presence of inclusions or voids which could be expected to be detrimental to bearing fatigue life. If these ten bearings from each group would have been excluded from the test groups as "inferior" bearings, the fatigue life results would appear as in figure 6. In figure 6, Weibull plots for the remaining 17 bearings in each of the two groups are shown. There are only three and five inner-race fail-

ures to be considered for the baseline and prestressed groups, respectively. It can be seen, however, that the statistical lives of the groups without the "inferior" bearings are no better than the lives of the groups of 27 bearings each. Five of these eight bearings had definite evidence of fatigue spall initiation at surface indentations. The occurrence of these surface initiated failures contributed significantly to the statistical results.

Of the fifteen failed inner races in both groups of 27 bearings each only two had spalls that appeared to be subsurface initiated. The remaining failed inner races either had definite evidence of spalls initiating at surface indentations or no evidence to indicate spall initiation source.

Typical spalls showing evidence of surface indentation initiation are shown in figures 7(a) and (b). The indentation (arrow) is seen at the leading edge of the spall. These indentations were apparently introduced during fatigue testing by foreign particles in the test apparatus or lubrication system. They definitely were not present prior to testing, since the visual inspection at ×30 would have disclosed them.

Further details of surface indentation initiation of fatigue cracks are shown in figures 7(c) and (d). Here microcracks have formed at the trailing edge of the indentation. This type of spall initiation has also been reported in [4, 5, and 25].

Metallurgical Analysis

A detailed appraisal of the magnetic perturbation data indicates that good correlation exists between the magnetic perturbation signal

and inclusion location and size. Each void signature region was metallurgically examined. In each case an inclusion was found. The data of table I are details on the sectioned specimens. Race number 131 failed at the signal location, and the inclusion was not found, but was assumed to have spalled out. Races number 11 and 116 with large opposite polarity signatures were sectioned to establish the source of these signatures. Initial optical examination of the raceway surfaces in the vicinity of these signal locations revealed no local surface alternations. The subsequent sectioning operation likewise failed to show any microscopically detectable flaw or anomalous condition, even though the same precision sectioning procedure (used to confirm all void signals) was followed.

Figures 8 and 9 show the good correlation between the signatures and the corresponding inclusions found by sectioning. Note the cracks apparently initiated by the fatigue testing on race number 3 in figure 8.

Peak separation of signatures as shown schematically in figure 10 can readily be used to predict inclusion depth. The linear relation between peak separation and defect depth is shown in figure 11. Races number 23 and 74 signal sources were identified as planar sulfide sheets [12], and this may possibly be the reason the depth indication is slightly in error.

Races number 24 and 130 provided the best example of the potential inherent in magnetic perturbation inspection of bearings to predict the precise point of failure. These two cases are detailed in figures 12 and 13. Note in particular (fig. 12) the 0.0068-centimeter (0.0027-in.) diameter nucleating inclusion, preserved within the spall region, which

caused the failure of race number 24. This inclusion could be viewed effectively only by means of polarized light. Although the inclusion responsible for nucleating the failure shown in figure 13 was lost during some phase of spalling, there obviously exists excellent correlation between the signal site at 308° and the leading edge of the spall. Close optical inspection of the leading edges of both spalls (24 and 130) showed no evidence of indentations. It is significant that not only were these the two largest signals of all races, 67 millivolts for number 24, and 58 millivolts for number 130, but also the axial locations (7.7° and 357.5°, respectively) were well within the zone of resolved shearing stresses.

Figure 14 shows the locations, relative size, and depth of the inclusions that were confirmed by metallurgical sectioning, relative to the race surface and the highly stressed zone of resolved shearing stresses. This zone was approximately located by suitably etching the sectioned races. Races number 3 (fig. 8) and 6 have cracking at the inclusions although a spall had not yet developed. The inclusions in races number 23 and 74 were identified as planar sulphide sheets. The inclusions in races number 85 (fig. 9) and 25 were hard oxide or silicate inclusions surrounded by softer sulfide particles. The association of the sulphides in these four specimens tend to reduce the severity of the inclusions [26 and 27]. The absence of spalls or cracks at these locations could be related to the presence of the sulphides.

CONCLUDING REMARKS

There was excellent correlation between the magnetic perturbation signatures and the position of inclusions as determined by the precision metallurgical sectioning. However, the results of this study indicate that exclusion of bearings as a result of the magnetic perturbation data would not have altered the statistical lives of the groups of bearings tested. The occurrence of the surface indentation initiated failures significantly affected the evaluation of the inspection technique. However, these results do show that failures which may be inclusion or subsurface defect initiated may be eliminated by detecting the potential fatigue nuclei prior to bearing assembly using the magnetic perturbation technique. The use of this nondestructive inspection technique may be warranted where extremely high reliability is required.

It should be recalled that the bearings used in this study were air-melted, vacuum-degassed steel. Consumable-electrode vacuum-melted steels or the double vacuum melted steels are used for most applications where high reliability is required. These vacuum-melted steels have fewer nonmetallic inclusions that would be located by this inspection technique.

SUMMARY

A magnetic perturbation inspection technique was used to nondestructively detect subsurface nonmetallic inclusions in the inner races of 207-size, deep-groove ball bearings. The bearings were fatigue tested at 2750 rpm under a radial load of 5860 newtons (1320 lb). The

inner races were subsequently sectioned at fatigue spall locations and at magnetic perturbation signal locations. The following results were obtained:

1. Good correlation was found between magnetic perturbation signal characteristics and the location, size, and depth of nonmetallic inclusions.

2. The two largest magnetic perturbation signals corresponded precisely with the only observed inclusion nucleated fatigue failures.

3. Exclusion of those bearings that had significant magnetic perturbation signals did not alter the statistical life of the bearings tested. This result was significantly influenced by the occurrence of many surface indentation initiated failures.

ACKNOWLEDGEMENT

The magnetic perturbation inspection and metallurgical sectioning of the inner races were performed by Southwest Research Institute under NASA contract NAS3-13944 under the direction of J. R. Barton and J. Lankford, Jr. The bearing fatigue tests were conducted by MRC Division of TRW, Inc. under NASA contract NAS3-10184.

REFERENCES

1. Jones, A. F.: Metallographic Observations of Ball Bearing Fatigue Phenomena. Symposium on Testing of Bearings, ASTM, 1947, pp. 35-52.
2. Carter, T. L.; Butler, R. H.; Bear, H. R.; and Anderson, W. J.: Investigation of Factors Governing Fatigue Life with the Rolling-Contact Fatigue Spin Rig. ASLE Trans., vol. 1, No. 1, April 1958, pp. 23-32.
3. Carter, T. L.: A Study of Some Factors Affecting Rolling-Contact Fatigue Life. NASA TR R-60, 1960.
4. Martin, J. A. and Eberhardt, A. D.: Identification of Potential Failure Nuclei in Rolling-Contact Fatigue. Journal of Basic Engineering, Trans. ASME, Series D, Vol. 89, No. 4, Dec. 1967, pp. 932-942.
5. Littman, W. E. and Widner, R. L.: Propagation of Contact Fatigue from Surface and Subsurface Origins. Journal of Basic Engineering Trans, ASME, Series D., Vol. 88, No. 3, Sept. 1966, pp. 624-636.
6. McMaster, R. C., ed.: Nondestructive Testing Handbook, Vols. I and II. Society for Nondestructive Testing, Roland Press, 1963.
7. Betz, C. E.: Principles of Magnetic Particle Testing. Magnaflux Corp., 1967.
8. Barton, J. R. and Kusenberger, F. N.: Magnetic Perturbation Inspection to Improve Reliability of High Strength Steel Components. Paper 69-DE-58 presented at ASME Design Engineering Conf., New York, May 1969.
9. Gardner, C. G. and Barton, J. R.: Recent Advances in Magnetic Field Methods of Nondestructive Evaluation for Aerospace Applications. Paper presented at 35th Meeting of the Propulsion and Energetics Panel, Advisory Group for Aerospace Research and Development, London, April 1970.

10. Barton, J. R. and Kusenberger, F. N.: Fatigue Damage Detection. STP 495, ASTM, 1971, pp. 193-208.

11. Lankford, J. and Francis, P. H.: Magnetic Field Perturbation Due to Metallurgical Defects. Int. J. NDT, Vol. 3, 1971, pp. 77.

12. Barton, J. R. and Lankford, J.: Magnetic Perturbation Inspection of Inner Bearing Races. NASA CR-2055, May 1972.

13. Barton, J. R.; Lankford, J.; and Hampton, P. L.: Advanced Non-destructive Testing Methods for Bearing Inspection. SAE Paper No. 720172, Automotive Engineering Congress, Detroit, Mich., Jan. 1972.

14. Parker, R. J., and Zaretsky, E. V.: Effect of Residual Stresses Induced by Prestressing on Rolling-Element Fatigue Life. NASA TN D-6995, Oct. 1972.

15. Kittel, C.: Physical Theory of Ferromagnetic Domains. Reviews of Modern Physics, Vol. 21, No. 4, Oct. 1949.

16. Bozarth, R. M.: Ferromagnetism. New York, D. Van Nostrand Co., Inc. 1951.

17. Williams, H. J. and Shockley, W.: A Simple Domain Structure in an Iron Crystal Showing a Direct Correlation with the Magnetization. Physical Review, Vol. 75, No. 1, Jan. 1949.

18. Goodenough, J. B.: A Theory of Domain Creation and Coercive Force in Polycrystalline Ferromagnetics. Physical Review, Vol. 95, No. 4, Aug. 1954.

19. Kittel, C.: Theory of the Formation of Powder Patterns on Ferromagnetic Crystals. Letters to the Editor, Physical Review, Vol. 76, No. 10, Nov. 1949.

20. Bates, L. F. and Neale, F. E.: A Quantitative Study of the Domain Structure of Single Crystals of Silicon-Iron by the Powder Pattern Technique. Proc. of Physical Society, Vol. 63.

21. Graham, C. D., Jr. and Neurath, P. W.: Domain Wall Orientations in Silicon-Iron Crystals. J. of Applied Physics, Vol. 28, July 1957.

22. Stewart, K. H.: Domain Wall Movement in a Single Crystal. Proc. of Physical Society, LXIII, 7-A.

23. Gardner, C. G.; Matzkanin, G. A.; and Davidson, D. L.: The Influence of Mechanical Stress on Magnetization Processes and Barkhausen Jumps in Ferromagnetic Materials. Int. J. of Nondestructive Testing, Gordon and Breach, Great Britain, Vol. 3, 1971, pp. 131-169.

24. Gardner, C. G.; Matzkanin, G. A.; and Lankford, J.: Influence of Stress and Plastic Deformation on the Barkhausen Effect in Silicon-Iron. Presented at Symposium on Advanced Nondestructive Testing Techniques, AAMRC, Watertown, Mass., sponsored by ARPA and AMMRC, June 1971.

25. Leonard, L.; Martin, J.; and Choman, L.: Special Report on Surface and Subsurface Observations of Endurance Tested 6309-Size Bearings. SKF Report AL69M025, Oct. 1969.

26. Brooksbank, D. and Andrews, K. W.: Stresses Associated With Duplex Oxide-Sulphide Inclusions in Steel. Journal of the Iron and Steel Institute, June 1970, pp. 582.

27. Lyne, C. M. and Kasak, A.: Effect of Sulphur on the Fatigue Behavior of Bearing Steel. Trans. of the ASM, Vol. 61, 1968, pp. 10.

TABLE 1. - CORRELATION OF MAGNETIC PERTURBATION SIGNATURES AND PRECISION METALLURGICAL SECTIONING

Race' number	Hours	Angle, deg		Post-endurance run			Pre-endurance run			Peak separation, cm $\times 10^{-3}$ (in. $\times 10^{-3}$)	Defect depth, cm $\times 10^{-3}$ (in. $\times 10^{-3}$)	Defect size, cm $\times 10^{-3}$ (in. $\times 10^{-3}$)
		Circ.	Axial	Amplitude, mV		Peak / background	Amplitude, mV		Peak / background			
				Void	Opposite		Void	Opposite				
[a]3	4 000	5	3.5	40		1.7/1	39		3/1	4.6 (1.8)	1.9 (0.75)	3.8 (1.50)
6P	10 000	312	347.0	28		2.5/1	53		5/1	4.6 (1.8)	1.0 (0.40)	2.54 (1.00)
23P	10 000	327	7.7	50		2.5/1	22		4/1	4.6 (1.8)	2.54 (1.00)	3.8 × 6.3 × 0.5 (1.5 × 2.5 × 0.2)
[b]24	1 903	9	7.7	--		-----	67		6/1	5.6 (2.2)	----------	6.8 (2.70)
25P	10 000	195	352.2	34		1.5/1	30		2.5/1	7.1 (2.8)	6.1 (2.40)	2.8 (1.10)
69P	10 000	50	23.5	44		2/1	38		4/1	5.3 (2.1)	2.16 (0.85)	3.05 (1.20)
74	4 000	226	2.5	60		5.5/1	25		2/1	7.1 (2.8)	7.6 (3.00)	2.5 × 11.5 × 0.25 (1.0 × 4.5 × 0.1)
85	4 000	305	347.0	52		4/1	49		7/1	6.1 (2.4)	3.8 (1.50)	7.0 (2.75)
120P	10 000	288	357.5	42		2/1	47		3/1	5.0 (2.0)	1.5 (0.60)	2.3 (0.90)
[b]130	1 333	308	357.5	--		-----	58		6/1	6.6 (2.6)	----------	----------
11P	10 000	315	[c]352.2 to 18.2		115	7/1		55	6/1	24.4 (9.6)	----------	----------
116	1 969	55	[c]2.5 to 18.2		92	4.5/1		30	4/1	---------	----------	----------

[a]Cracking at inclusion.

[b]Failed at signal.

[c]Range over which opposite polarity signal persisted.

P prestressed during run-in cycles.

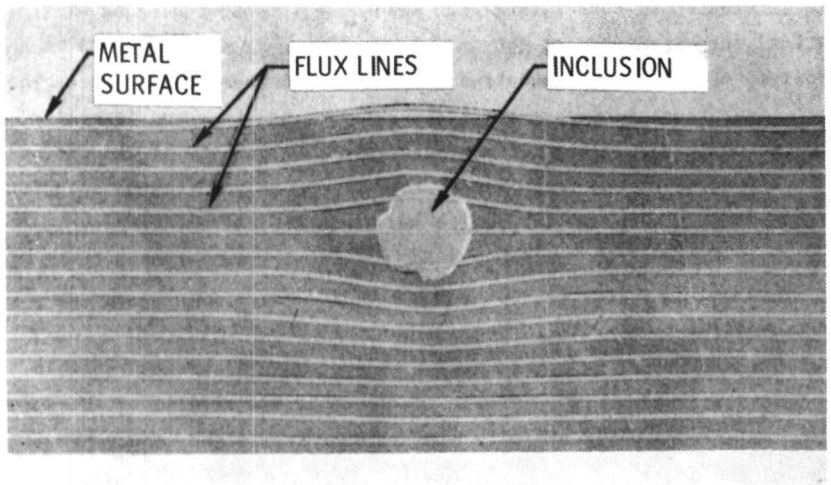

Figure 1. - Perturbations in magnetic flux caused by inclusion in ferromagnetic material.

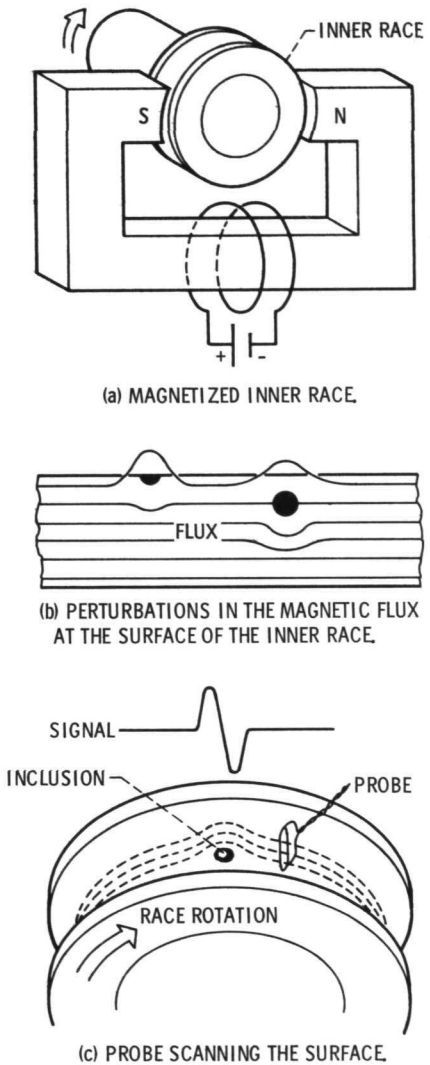

Figure 2. - Schematic illustration of magnetic perturbation method applied to bearing inner race.

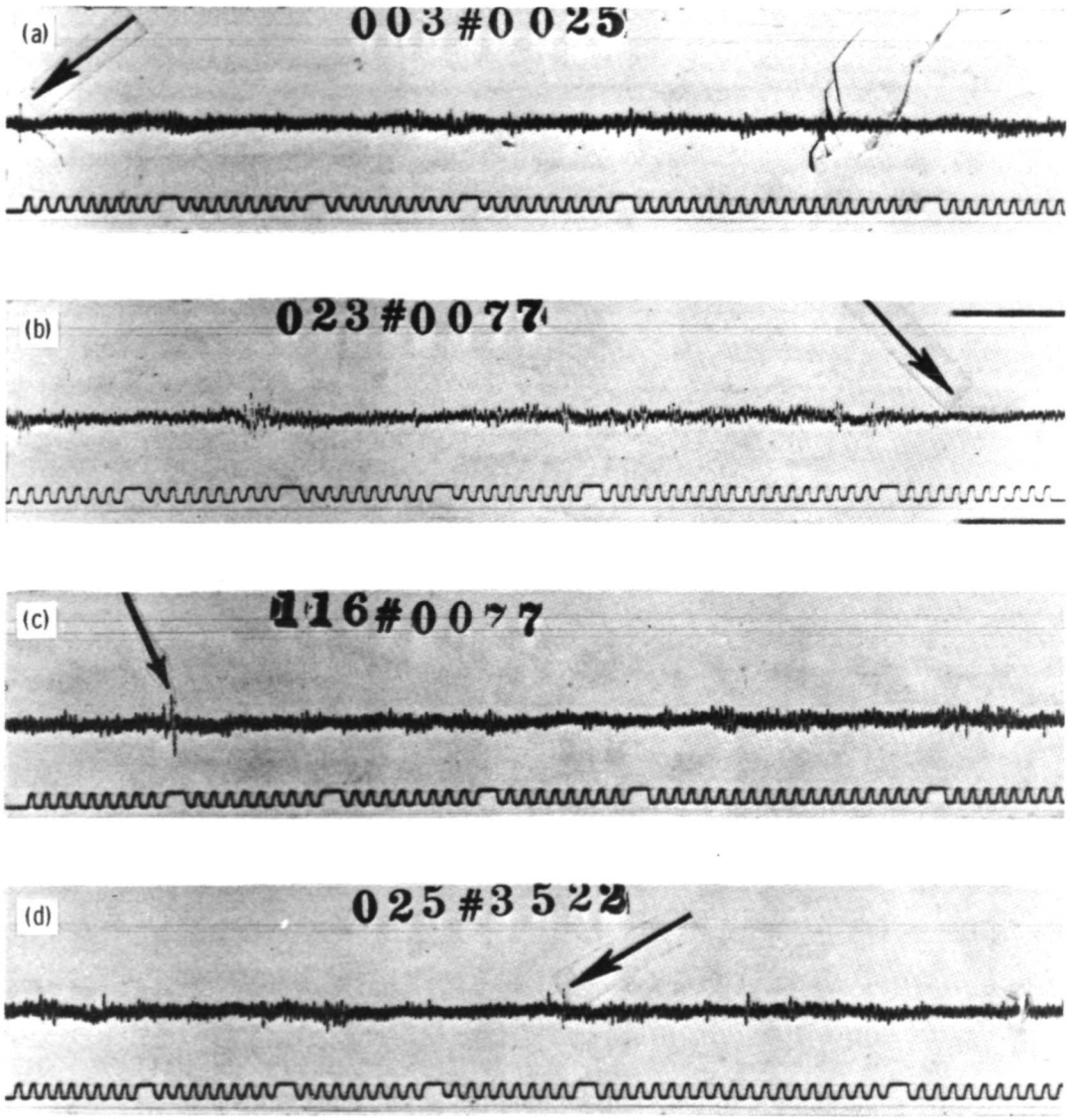

Figure 3. - Inspection records with typical signals (prior to endurance testing). Signal in (c) is of opposite polarity.

E-7549

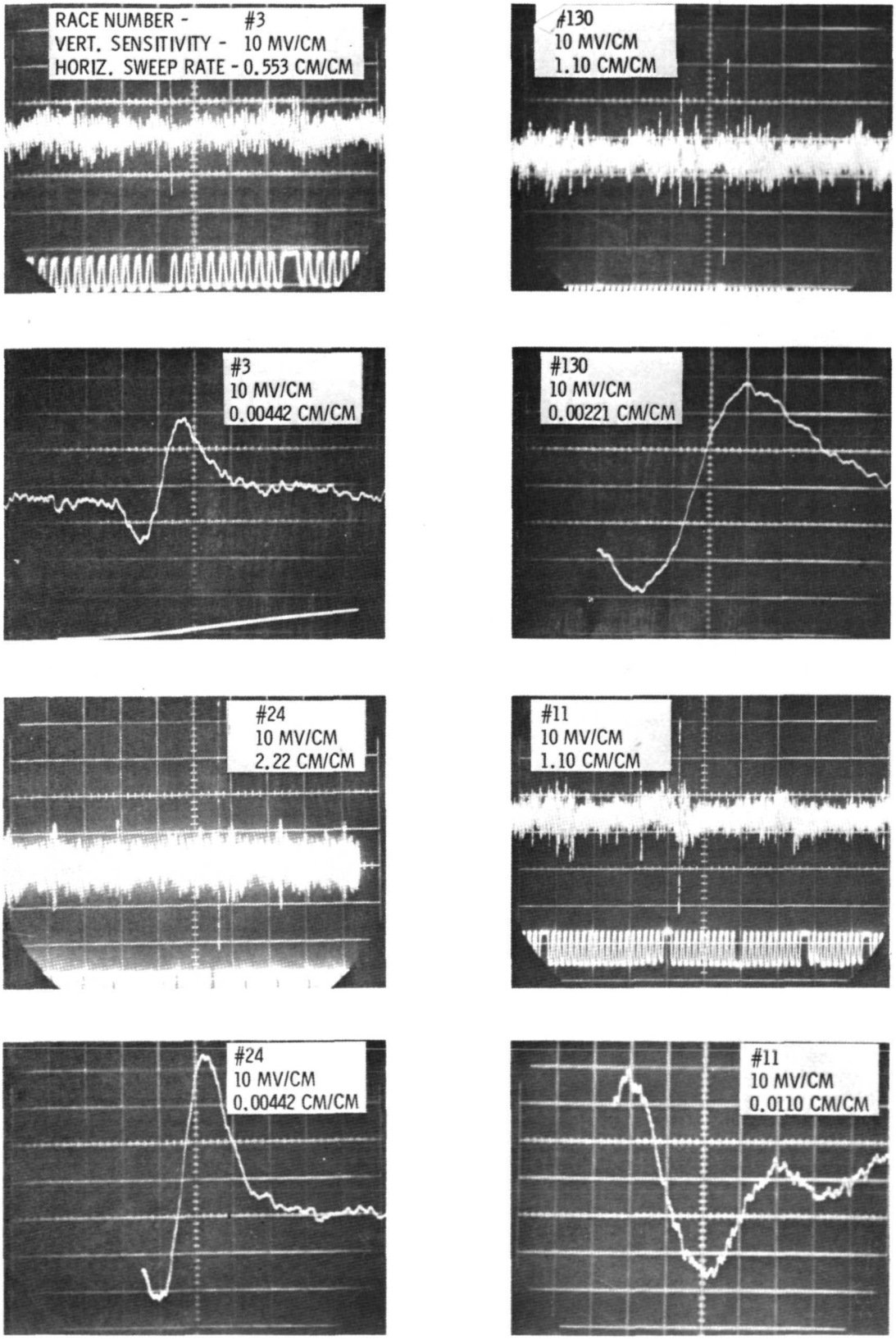

Figure 4. - Selected records with expanded time base.

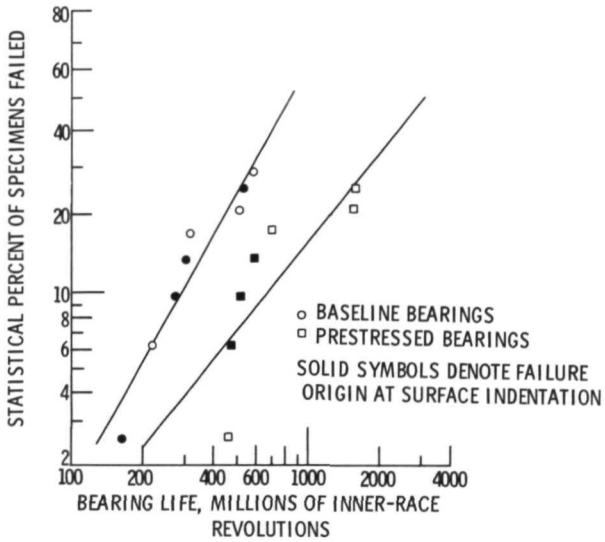

Figure 5. - Results of fatigue tests with 207-size ball bearings tested at a radial load of 5860 newtons (1320 lb) and a shaft speed of 2750 rpm with a superrefined naphthenic mineral oil.

E-7549

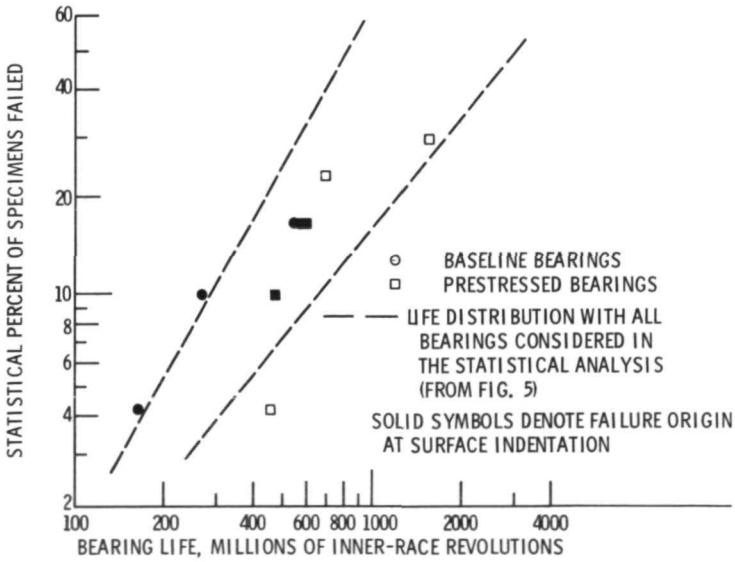

Figure 6. - Fatigue test results that would be obtained by excluding the bearings which had significant signals from magnetic perturbation inspection of their inner races.

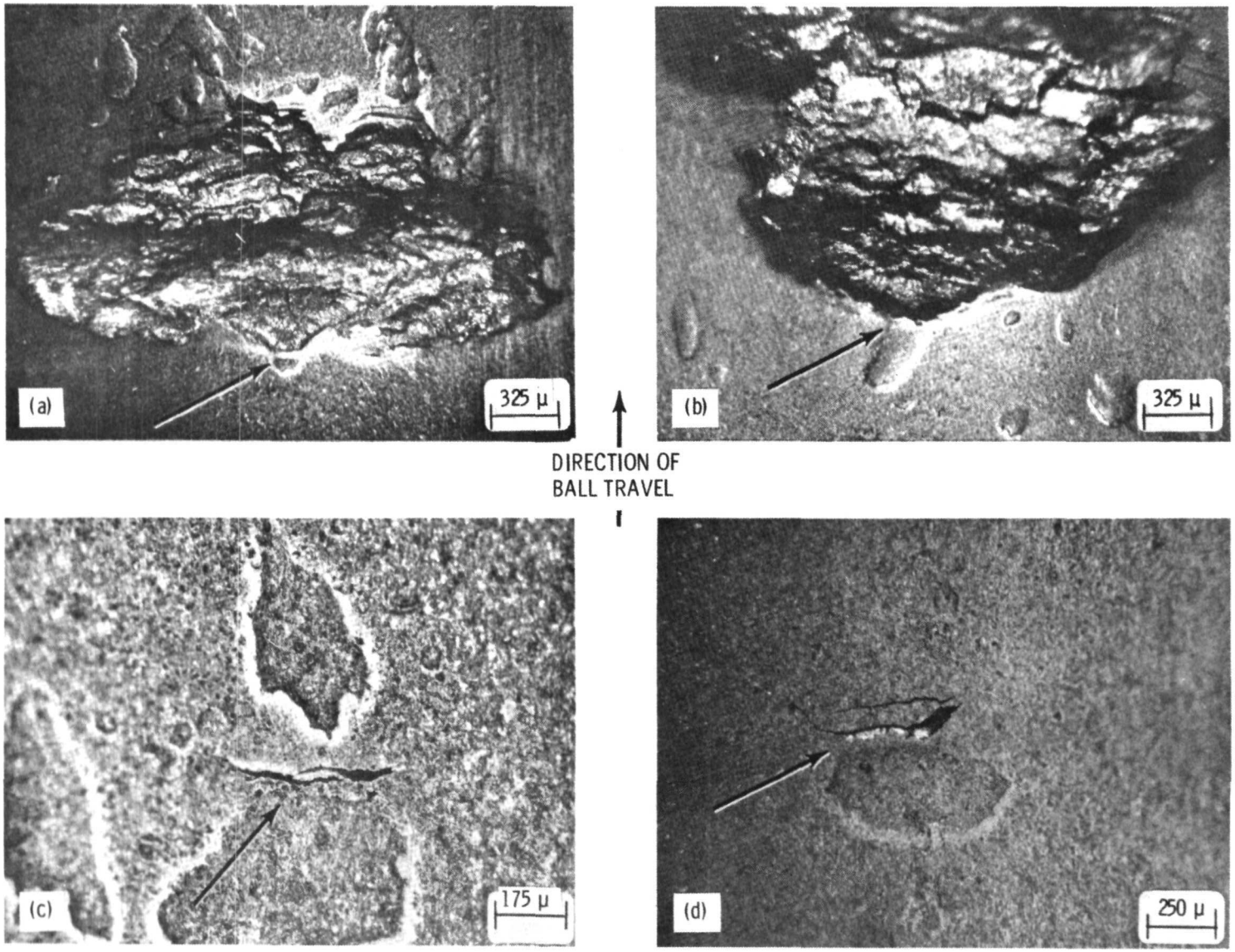

Figure 7. - Spalls (a-b) and pre-spall cracking (c-d) at surface indents. (Arrows indicate spall formation at trailing edge of indents).

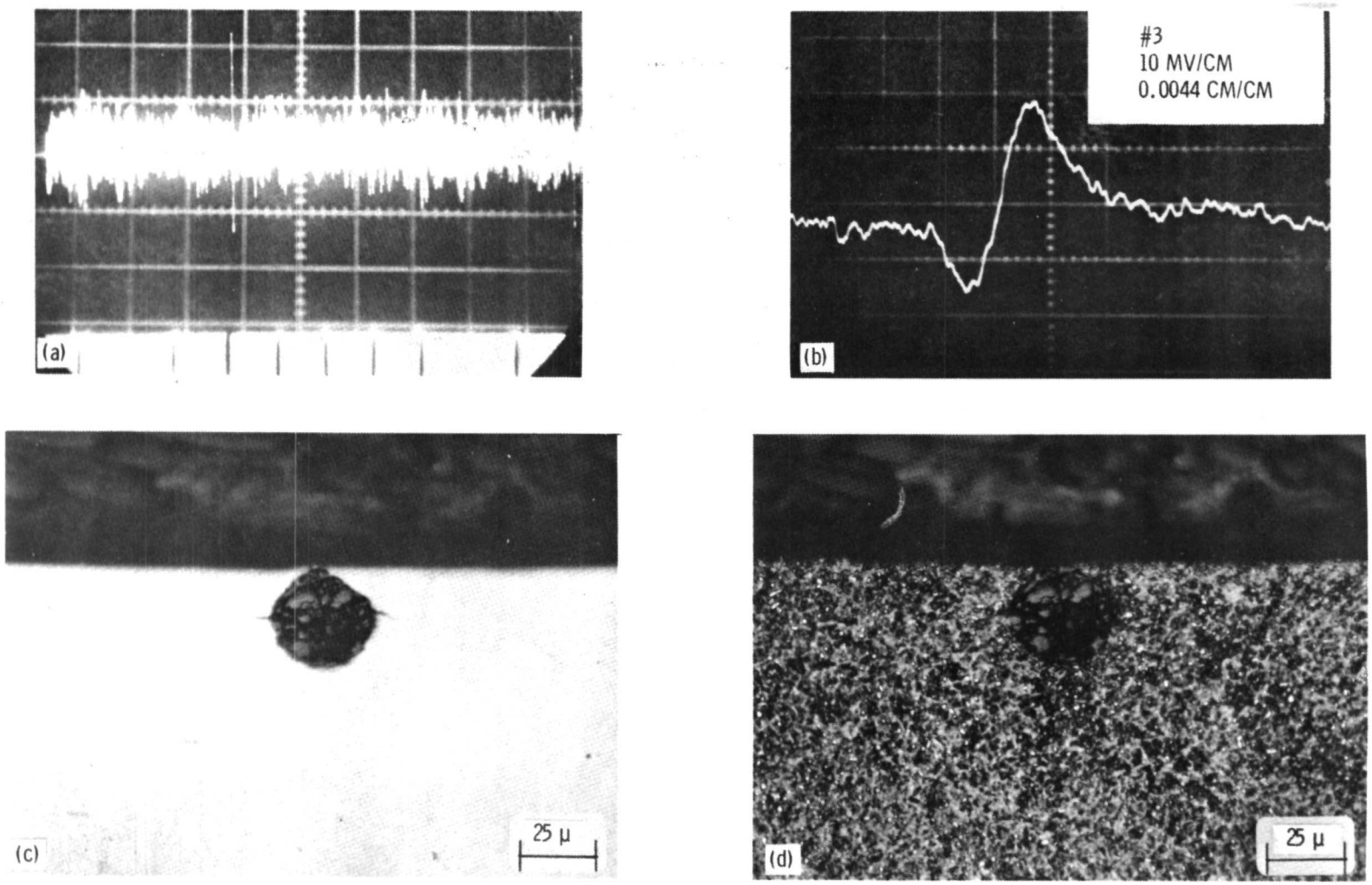

Figure 8. - Race #3 defect signal at 5^0 and corresponding defect. (Note cracking evident in unetched view (c).

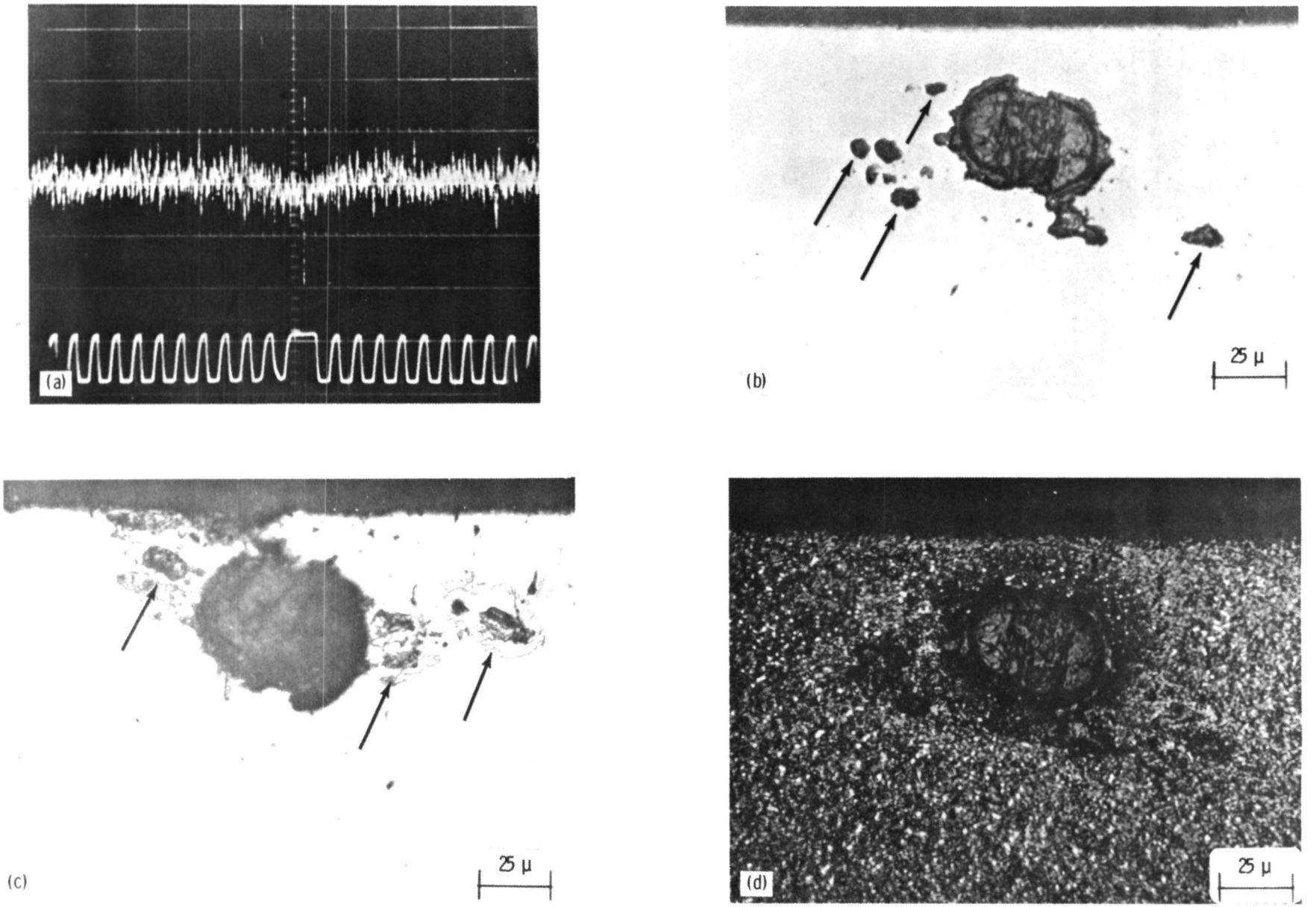

Figure 9. - Race #85 defect signal at 305° and corresponding defect. (Note sulfide particles (arrows) about the inclusions in (b) and (c), two sections separated by 12.5 μ).

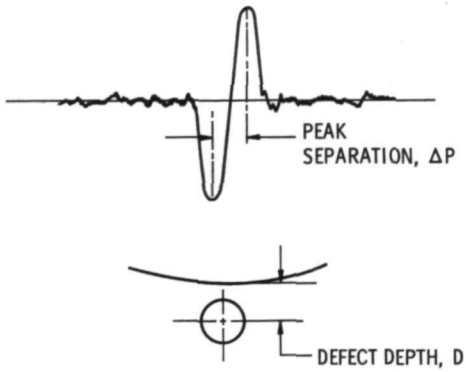

Figure 10. - Schematic view of magnetic perturbation signal having peak separation ΔP caused by defect at depth D.

E-7549

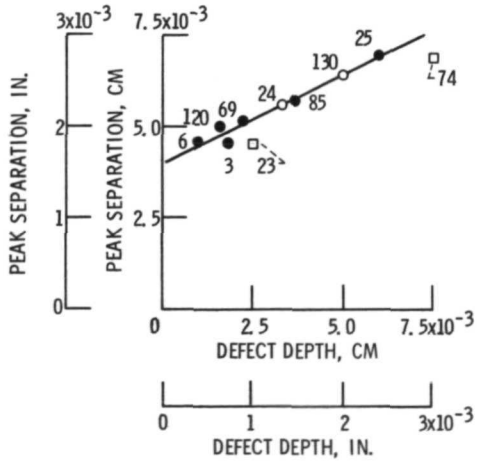

Figure 11. - Plot of peak separation versus depth for several defects.

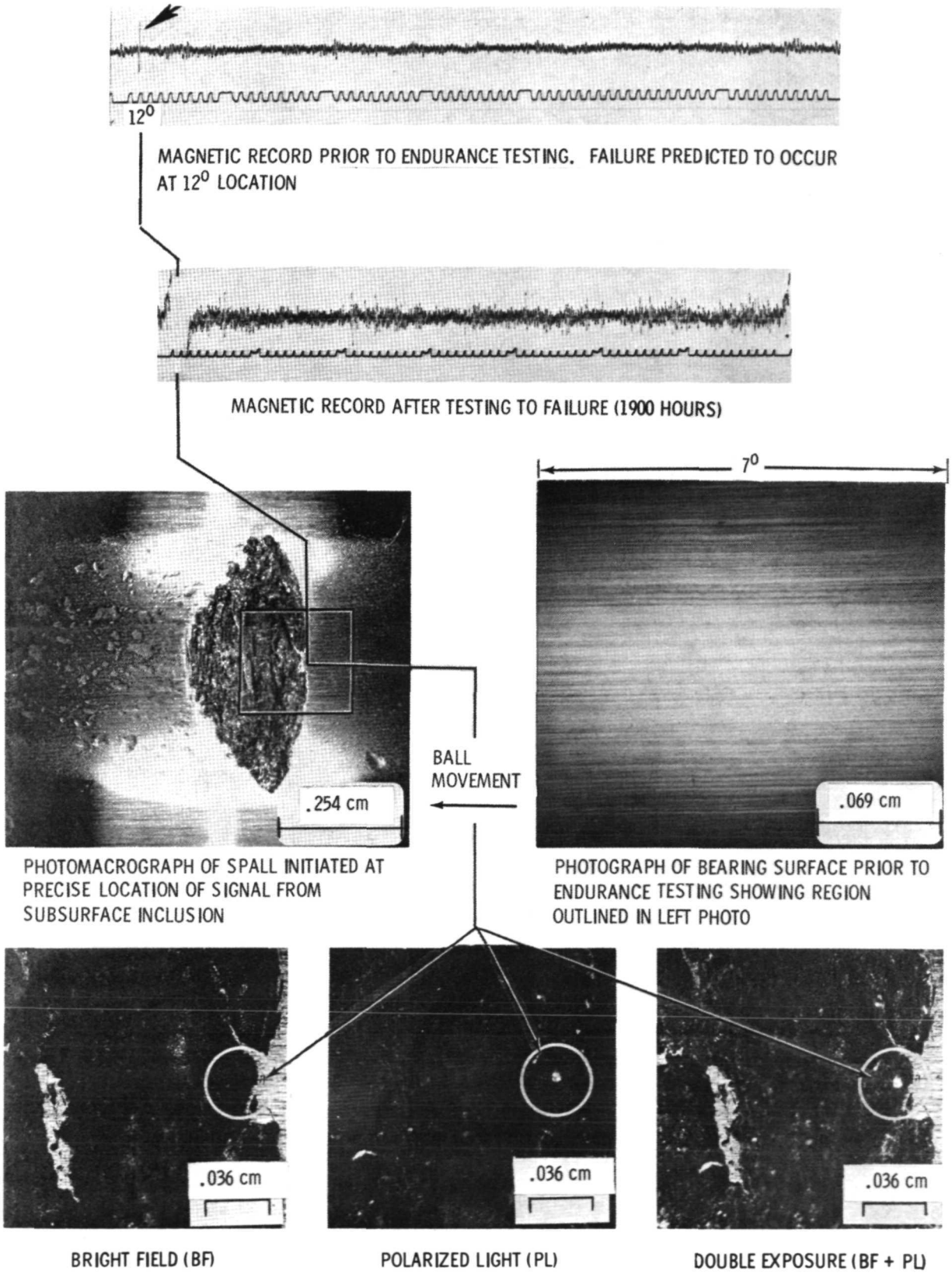

Figure 12. - Inclusion failure initiated at subsurface in bearing #24.

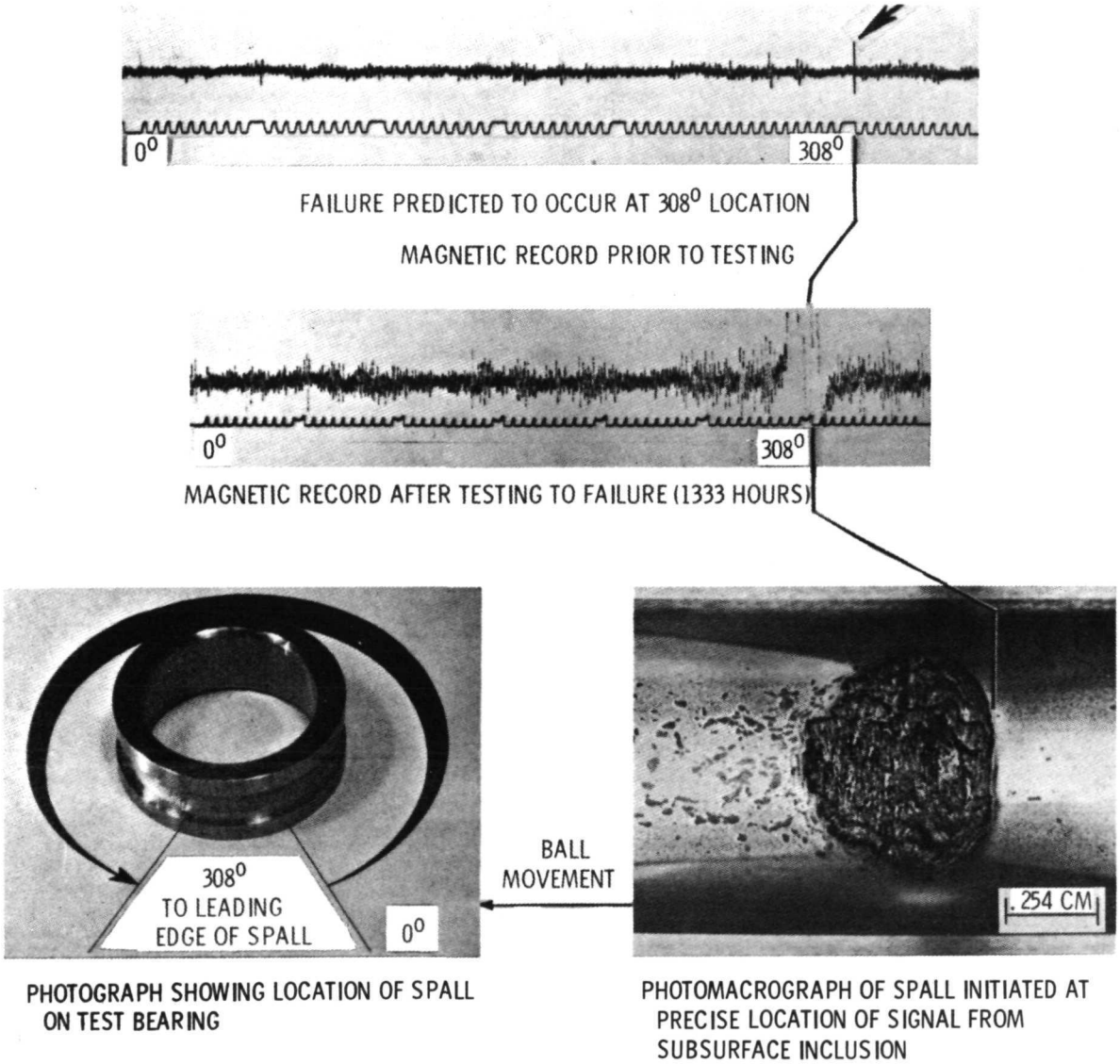

Figure 13. - Spall at predicted site in bearing #130.

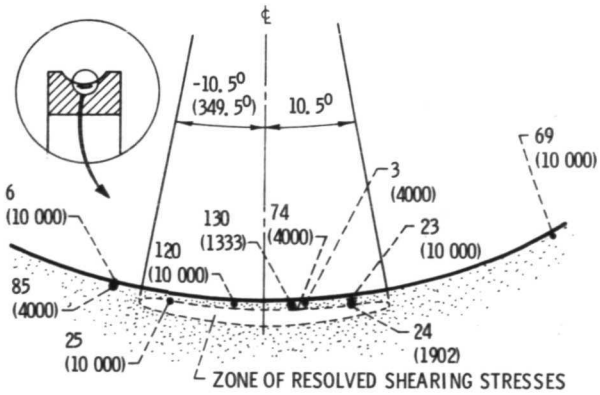

NASA-Lewis

Figure 14. - Schematic showing defect locations and subsurface zone of resolved shearing stresses (life in hours in parentheses).

E-7549